

Radiative and Nonradiative Recombination at Neutral Oxygen in *p*-Type GaP

J. M. Dishman

Bell Telephone Laboratories, Murray Hill, New Jersey 07974

(Received 6 July 1970)

A new near-infrared photoluminescence band attributed to the radiative capture of free holes by neutral oxygen donors has been observed in *p*-type zinc- and oxygen-doped GaP. The new emission is observed at temperatures above 70 °K and consists of a no-phonon line at 1.453 ± 0.002 eV and several-phonon replicas resulting from phonon energies of 23 and 52 meV. This free-to-bound luminescence is observed concurrently with the 1.40-eV luminescence band due to O-Zn donor-acceptor pair recombination, and is seen to be the dominant radiative recombination mechanism at neutral oxygen above 120 °K. The temperature dependence of the total near-infrared luminescence from neutral oxygen is found to be a strong function of zinc doping. In particular, lightly doped *p*-type crystals show an increasing luminescence quantum efficiency as the temperature is raised from 60 to 300 °K, while the more heavily doped *p*-type samples show a quenching of the luminescence with increasing temperature. These effects are explained on the basis of several nonradiative Auger processes involving the electron trapped at neutral oxygen.

I. INTRODUCTION

The luminescent properties of the deep oxygen donor in GaP have recently received considerable attention. Dean, Henry, and Frosch¹ have shown that near-infrared luminescence (~ 1.40 eV) is produced at low temperature (~ 4 °K) from recombination of electrons on neutral oxygen donors with holes trapped on distant shallow acceptor atoms (Zn, Cd, and C). From analysis of the individual donor-acceptor (DA) pair lines, they deduce the ionization energy of the O donor to be 895 meV.² Dean and Henry³ have also observed infrared luminescence (~ 0.84 eV) due to electron capture at ionized oxygen donors. Sharp structure is observed resulting from transitions between a shallow excited state and the ground state of the O donor. To explain the quenching of this luminescence with increasing acceptor concentration they suggest the existence of a nonradiative two-center Auger process in which the energy of the captured electron is given up to a hole on a nearby neutral acceptor. They have also proposed that Auger recombination of excitons bound to neutral O donors may explain the more rapid saturation of the 1.40-eV emission with excitation intensity relative to the 0.84-eV band at ~ 2 °K.

The present paper describes a new infrared emission band (~ 1.45 eV) resulting from the capture of free holes by neutral oxygen donors.⁴ The no-phonon (NP) line resulting from the free-to-bound (FB) transition is observed, as well as two-phonon replicas. Sharp structure due to FB recombination is found only in weakly compensated regions of lightly zinc-doped ($\sim 10^{17}$ cm⁻³) crystals of GaP(Zn, O) at temperatures above 70 °K. At lower temperatures, DA recombination dominates the infrared luminescence. As the temperature is raised the FB emis-

sion appears as a sharp line on the high-energy tail of the DA luminescence. The FB luminescence grows rapidly relative to the DA band and becomes the dominant infrared emission above ~ 90 °K. Although no sharp FB structure is observed in more heavily zinc-doped samples, it is concluded on the basis of Fermi-Dirac statistics and a simple kinetic model that the FB transition is the primary radiative recombination mechanism at neutral O donors in GaP in all *p*-type material above ~ 120 °K. Confirming this idea is the observation that the room-temperature infrared emission bands (~ 1.36 eV) in all *p*-type crystals of GaP (Cd, O) and GaP (Zn, O) are identical.

A marked contrast is observed in the temperature dependence of the total infrared emission band (FB + DA) as a function of Zn doping in *p*-type crystals. In the lightly doped crystals, the infrared luminescent efficiency *increases* as the temperature is increased from 60 to 300 °K. For the more heavily doped samples, however, the infrared efficiency decreases with increasing temperature. To explain these results the existence of at least two (and possibly three) nonradiative Auger mechanisms is postulated. At low temperatures, nonradiative recombination at neutral O donors can proceed by means of a three-center Auger process in which the energy released in a DA pair transition is taken up by a second hole bound to a nearby neutral acceptor. At higher temperatures, where a large fraction of the acceptors are ionized, a single-center Auger mechanism is operative. In this process, the energy released when a free hole is captured by a neutral O donor is taken up by a second free hole, which is ejected deep into the valence band. Results of calculations⁵ of the recombination coefficients of these processes are presented and it is found that the

three-center Auger process is sensitive to the acceptor binding energy and to the plasma screening of the Coulomb potential by free holes. Hence, its strength is a strong function of Zn doping. It is this effect which apparently gives rise to the unusual variation with doping of the temperature dependence of the infrared luminescence.

II. SPECTRA

The GaP samples in which the new emission was observed were grown from Ga-rich solutions⁶ containing 0.007-mole% Zn and 0.02-mole% Ga₂O₃. Only selected regions of the crystals studied showed the new emission band. The luminescence was excited by 6328-Å radiation from a (5-mW) He-Ne laser, which photoneutralizes the ionized O donors by promotion of electrons from the valence band.⁷ The samples were mounted in a cold-finger Dewar, and both exciting and sampling optics were defocused so that changes in measured intensity due to changes in sample position with temperature were minimized. It is estimated that the relative intensities of spectra taken at different temperatures are determined to within $\pm 5\%$.

The resulting spectra as a function of temperature are shown in Fig. 1. At 60 °K, the luminescence is similar to the DA emission band observed by Dean *et al.*¹ at 4 °K (e.g., see Fig. 4 of Ref. 1). The NP band (composed of a number of unresolved pair lines) peaks at 1.392 ± 0.002 eV and is replicated by phonons of energy 19 and 45 meV. The 45-meV phonon energy is ≈ 2 meV lower than that observed at 4 °K.¹ The new structure is first observed at 70 °K as a small protrusion on the high-energy side of the pair band. At 76 °K the NP line at 1.453 ± 0.002 eV and a single phonon replica are further developed concurrent with a substantial broadening of the pair emission band. The new structure is fully developed at 87 °K, where at least two phonon replicas are resolvable in addition to the NP line. The phonon energies giving rise to the replicas correspond to 23 and 52 meV, respectively. These values are ≈ 5 meV higher in energy than the corresponding replicas for the pair emission.¹ This increase in phonon energy is thought to correspond to a change in the momentum conservation requirement in going from a pair to a FB transition.

Both the width and peak position of the 1.453-eV band argue for its identification as a FB transition. At 87 °K, the observed width of the NP line is approximately 28 meV, or $\approx 4kT$. This is a reasonable width for a FB transition, and arises as a consequence of the distribution of hole energies in the valence band. The threshold energy $h\nu_0$ for the FB transition can be calculated as the difference between the band gap E_g and the ionization energy E_O of the oxygen donor. If the oxygen-donor level remains fixed relative to the conduction band at the

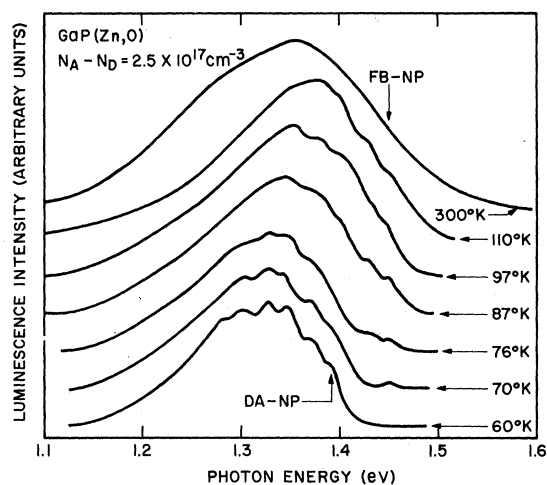


FIG. 1. Photoluminescence spectra from lightly zinc-doped GaP(Zn, O) as a function of temperature. The zero of each spectrum has been shifted for clarity, and corresponds to the position of the arrow denoting temperature. The NP energies for the free-to-bound and donor-acceptor pair transitions are designated by FB-NP and DA-NP, respectively.

value $E_O = 0.895$ eV¹ as a function of temperature, then at 87 °K taking $E_g = 2.331$ eV,⁸ we find $h\nu_0 = 1.436$ eV. On the other hand, if the oxygen level is tied to the valence band, then $h\nu_0 = 1.443$ eV. In either case the 1.453-eV emission peak is within $2kT$ of the expected FB threshold.

Evidence to be presented in Sec. III indicates that the O level is rigidly fixed relative to the valence band for $T < 87$ °K. As the temperature is raised from 87 to 110 °K the FB peak is observed to shift by approximately 3 meV to lower energies. Over the same temperature range the band gap decreases by approximately 6 meV.⁸ Thus, it appears that in this range the oxygen level is not rigidly tied to either band. Above 110 °K the infrared emission broadens into a single band with no resolvable structure (see Fig. 1). The peak of the band shifts from 1.370 eV at 110 °K to 1.356 eV at 300 °K, a shift of 14 meV as compared to a reduction of 60 meV in the bandgap⁸ over the same temperature interval. This smaller shift in the infrared band as compared to the band gap cannot necessarily be constructed to mean that the O level is tied to the valence band over this temperature range. The structureless infrared emission observed above 110 °K is presumably composed of a series of broadened phonon replicas of the FB transition, each of which broadens to higher energies as the temperature is raised, reflecting the change in the distribution of free-hole energies in the valence band. Thus, any shift in the energy threshold of the FB-NP transition to lower energies would be at least partially offset by the broadening of the NP line and each replica to higher energies.

Luminescence spectra from crystals grown from solutions containing 0.07-mole% Zn and 0.02-mole% Ga₂O₃ are shown in Fig. 2. (For convenience, since the total infrared band decreases with increasing temperature in this case, the spectra are ordered oppositely to the arrangement in Fig. 1.) Again at the lowest temperature, the DA pair emission is observed, except in this case the NP line peaks at 1.399 ± 0.002 eV, 7 meV higher than observed for the more lightly doped sample. This increase in energy can be attributed to the reduction in the binding energy of Zn acceptors with increased doping [see Eq. (15)]^{9,10} to broadening of the Zn level with doping, or to increased near-neighbor pairing. No sharp structure attributable to FB transitions is observed in this material. However, at 104 °K a shoulder appears on the infrared band corresponding in energy to the FB transition observed in the lightly doped crystals. The shoulder grows in intensity at 115 °K, and the vestiges of the NP-FB transition and two replicas can be made out by comparison with the 110 °K spectrum from the lightly doped sample (cf. Figs. 1 and 2). Above 115 °K, the infrared emission broadens rapidly to higher energies and becomes essentially identical in shape to that observed at corresponding temperatures in the lightly doped crystals. It is possible to conclude from this behavior that FB transitions are also the dominant source of the infrared emission in the more heavily doped crystals above ≈ 120 °K.

To justify this conclusion the relative strengths of the FB and DA luminescence can be straightforwardly calculated from Fermi-Dirac statistics and

a simple model of the recombination kinetics. The FB transition rate r_{FB} (in units of cm⁻³ sec⁻¹) due to hole capture by neutral oxygen donors is given by

$$r_{FB} = B_{FB} p N_O^0, \quad (1)$$

where B_{FB} is the capture coefficient, p is the free-hole density, and N_O^0 is the concentration of neutral oxygen donors. It is difficult to express the total DA pair recombination rate in a simple form because of the dependence of the rate on the spatial separation for each recombining pair.¹¹ This spatial dependence requires the use of ensemble averages in calculating the kinetics. Elaboration of this point is made in the Appendix, where it is shown that the DA recombination rate r_{DA} can be approximated by the form

$$r_{DA} = B_{DA} N_A^0 N_O^0, \quad (2)$$

where N_A^0 is the concentration of neutral acceptors. The generation rate of free holes and neutral oxygen donors resulting from the defocused below-band-gap He-Ne excitation used in these experiments is of order 5×10^{16} cm⁻³ sec⁻¹ (5 mW of 6328-Å radiation into a $\frac{1}{2}$ -cm-diam area, with an absorption coefficient⁷ of 2 cm⁻¹). The longest lifetime observed for the oxygen luminescence over the range of temperatures and zinc doping used in these experiments is ≈ 40 μsec.¹² Thus, we expect p and N_O^0 to be no greater than $\approx 2 \times 10^{12}$ cm⁻³ over this range. Since the oxygen concentration⁷ of the crystals studied is $\sim 10^{17}$ cm⁻³, saturation of the O donors by the photoexcitation is negligible. In addition, above 50 °K we may replace p in Eqs. (1) and (2) by its thermal equilibrium value p_0 . The temperature dependence of the relative magnitudes of the FB and DA transitions (r_{FB}/r_{DA}) is therefore determined by the ratio p_0/N_A^0 , modulated by the temperature dependence of B_{FB}/B_{DA} . As will be shown in Sec. IV, B_{DA} is expected to be temperature independent. In addition B_{FB} is only weakly temperature dependent, and is essentially independent of p_0 . Hence, the doping dependence of r_{FB}/r_{DA} is also determined primarily by p_0/N_A^0 . Using conventional semiconductor statistics¹³ and the charge neutrality relation

$$p_0 + N_D = N_A - N_A^0,$$

where N_D is the concentration of ionized donors, the temperature dependence of p_0/N_A^0 has been calculated for several doping conditions. The results are plotted in Fig. 3. At any temperature the ratio is largest for the lightly doped weakly compensated sample ($N_A - N_D = 2.5 \times 10^{17}$ cm⁻³). As a result of increased compensation ($N_A - N_D = 2.0 \times 10^{17}$ cm⁻³) the FB transition decreases in importance at lower temperatures. Experimentally it is found that only selected regions of the lightly Zn-doped crystals show sharp FB structure at ~ 90 °K. On the basis of Fig. 3, the observation of the NP-FB line in these

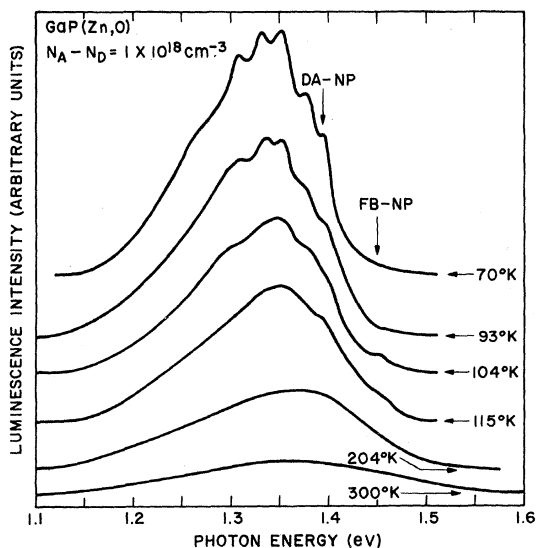


FIG. 2. Photoluminescence spectra from heavily zinc-doped GaP(Zn, O) as a function of temperature. Since the total infrared emission decreases with increasing temperature for this sample, the spectra are ordered oppositely from the arrangement in Fig. 1.

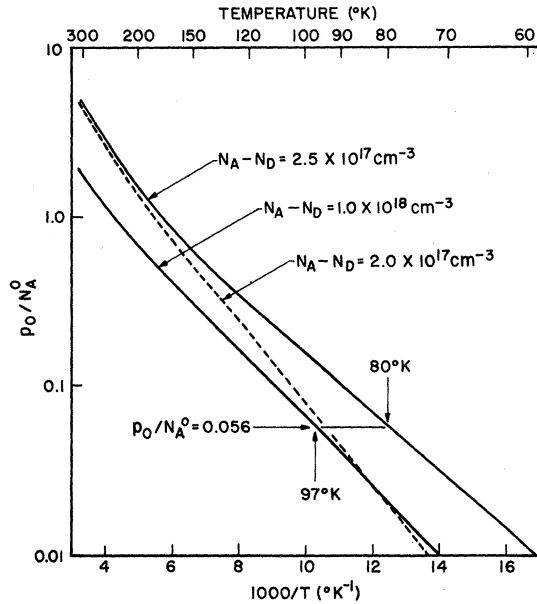


FIG. 3. The ratio p_0/N_A^0 of free holes to neutral acceptor atoms as a function of temperature, plotted for three doping levels using Eq. (3). The ratio of the FB recombination rate to the DA pair recombination rate is proportional to p_0/N_A^0 , and is largest for weakly compensated lightly zinc-doped samples. The arrows indicate that a value of $p_0/N_A^0 = 0.056$ at 80°K for the lightly zinc-doped weakly compensated sample is not achieved in the more heavily zinc-doped crystal until a temperature of 97°K is reached.

samples would appear to be correlated with local regions in which the residual donor concentration is depleted.¹⁴ For the more heavily Zn-doped sample ($N_A - N_D = 1.0 \times 10^{18} \text{ cm}^{-3}$) Fig. 3 also predicts a lower ratio of FB to DA luminescence, in agreement with the experimental findings. Thus, at $\approx 80^\circ\text{K}$ the ratio $r_{\text{FB}}/r_{\text{DA}}$ is ≈ 3 times lower than in the lightly doped weakly compensated crystal. If we assume that FB luminescence becomes comparable to DA luminescence for a ratio $p_0/N_A^0 = 0.056$ (see Fig. 3) as suggested by the $\approx 80^\circ\text{K}$ spectrum of the lightly Zn-doped sample (Fig. 1), then we expect FB recombination to become dominant in the more heavily doped sample at $\sim 100^\circ\text{K}$. This agrees with the spectral evidence in Fig. 2. On the basis of Fig. 3 it may be concluded that FB recombination is the dominant luminescent process at neutral oxygen above 120°K for all samples for which $N_A \leq 10^{19} \text{ cm}^{-3}$.

Before concluding the discussion of the spectral results it is worth noting similar effects observed in GaAs by Shah *et al.*¹⁵ Using much larger excitation densities ($\sim 10^{25} \text{ cm}^{-3} \text{ sec}^{-1}$) at lower temperature ($\sim 15^\circ\text{K}$) than in the present work, two "twin peaks" were observed in photoluminescence whose spectral characteristics were very similar to those

described here. Namely, the higher-energy band increased in intensity with increasing temperature, while the lower-energy band quenched. By noting that the ratios of the two bands followed a Boltzmann dependence independent of the position of the quasi-Fermi level ($p \gg p_0$ in their experiments), it was concluded that the higher-energy peak resulted from DA pair recombination between the first excited state of a shallow donor with distant acceptor impurities, whereas the lower-energy peak originated from conventional pair recombination involving only ground states. Their analysis also indicated that pair recombination involving the excited state of the donor should be favored in samples with the lowest donor concentration. This is comparable to the observation here of strong FB emission in lightly Zn-doped samples. The method used by Shah *et al.* to distinguish between FB and excited-state DA luminescence involved drawing a distinction between Fermi-Dirac and Boltzmann statistics in predicting the ratio of peak heights vs temperature. For the excitation densities used here, both sets of statistics predict the same behavior (cf. Fig. 3 of this work with Fig. 3 of Ref. 15), making such a distinction impossible.

To support the interpretation of the 1.453-eV luminescence as a FB transition, the spectra of a number of samples of GaP(Zn, O) and GaP(Cd, O) have been examined at room temperature. The broad infrared band observed in these crystals is found to be virtually identical, independent of the type of acceptor (Zn or Cd) and its concentration. This strongly suggests that the luminescence depends only on the donor level, i.e., it is FB emission. In Secs. III and IV additional support is drawn for this contention from the line shape of the emission and the temperature dependence of the total infrared luminescence band.

III. LINE SHAPE

From the application of detailed radiative balance, Blakemore¹⁶ has shown that a simple relation exists between the radiative capture cross section σ_{FB} of a localized impurity and its photoionization (or photoneutralization) cross section σ_α . Thus, if the spectral variation of σ_α is known, the spectral dependence of σ_{FB} can be found from the relation¹⁶

$$\sigma_{\text{FB}}(E) = \sigma_\alpha(h\nu) \frac{\beta^{-1} n^2 (h\nu)^2}{2c^2 m_v^* E} \quad (3)$$

In the above expression E is the energy of the hole (measured from the top of the valence band) prior to capture, $h\nu$ is the photon energy $h\nu = E_g + E - E_O$, β is the degeneracy of the ground state of the O donor, c/n is the speed of light in the crystal, and m_v^* is the valence-band effective mass. The spectral variation of the photoneutralization cross section $\sigma_\alpha(h\nu)$ for the O donor in GaP has been measured⁷

at 90 °K and the result near the low-energy threshold is shown in the inset of Fig. 4. The shape of this curve and its comparison with theoretical calculations¹⁷ is discussed elsewhere.⁷ For our purpose, the spectral variation of σ_α is used in Eq. (3) in order to calculate the shape of the 1.453-eV emission line (at 87 °K), which is determined from the relation

$$r_{\text{FB}}(h\nu) \approx p_0(E)v(E)\sigma_{\text{FB}}(E)N_O^0. \quad (4)$$

In Eq. (4), $p_0(E)$ is the thermal equilibrium concentration of free holes with energy E , and $v(E) = (2E/m_v^*)^{1/2}$ is the electron thermal velocity. The free-hole density $p_0(E)$ is itself a product of the density of states $g(E) \propto E^{1/2}$ and the thermal-equilibrium Fermi factor $f(E) \approx e^{(\varphi_0 - E)/kT}$ (φ_0 is the thermal-equilibrium Fermi level, which by the choice of origin is negative). The spectral variation of r_{FB} is therefore given by

$$r_{\text{FB}}(h\nu) \propto \sigma_\alpha(h\nu)(h\nu)^2 e^{(\varphi_0 - E)/kT}. \quad (5)$$

Taking $\varphi_0 = -43.5$ meV appropriate to $N_A - N_D = 2.5 \times 10^{17} \text{ cm}^{-3}$ at 87 °K, one obtains from Eq. (5) the calculated NP line shown by the full curve in Fig. 4. Using this shape for the FB emission line, the contributions of the first two-phonon replicas have been subtracted from the 87 °K spectrum in Fig. 1. The resulting experimental NP line is shown by the open circles in Fig. 4. Agreement with the calculated curve is excellent, adding fur-

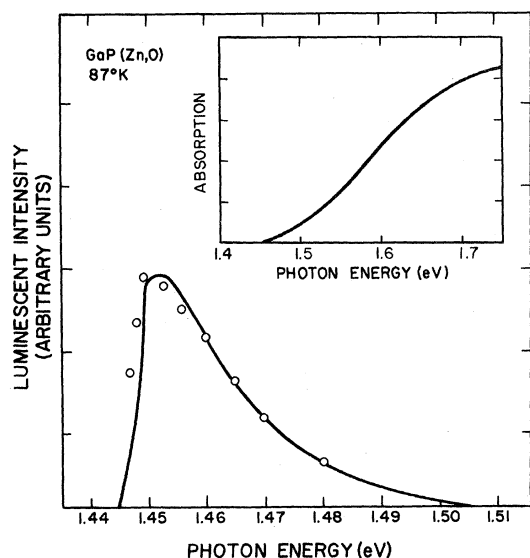


FIG. 4. Comparison of experimental and calculated line shapes for the NP-FB transition. The solid curve is calculated using Eq. (5) and the photoneutralization spectrum shown in the inset. The open circles are obtained by using the calculated shape to subtract the phonon replicas from the 87 °K spectrum in Fig. 1, as explained in the text.

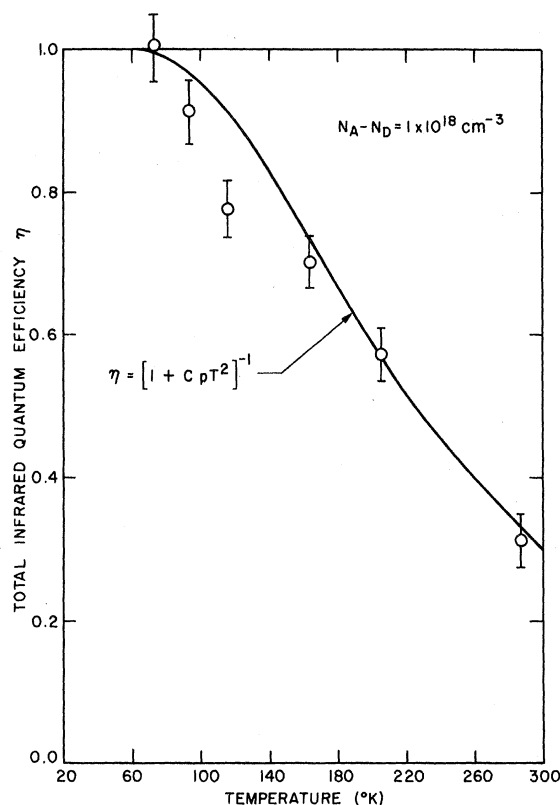


FIG. 5. Temperature variation of the total infrared emission from the heavily zinc-doped sample. The open circles represent the relative areas under the spectra in Fig. 2. The solid curve is plotted using Eq. (11), with $C = 3.2 \times 10^{-23} \text{ cm}^3 \text{ } ^\circ\text{K}^{-2}$.

ther support to the interpretation of the 1.453-eV emission as a FB transition.

The energy threshold $h\nu_0 = 1.445$ eV (obtained from the absorption curve in Fig. 4) predicts an ionization energy for the oxygen donor of $E_O = 886$ meV at 87 °K. The decrease in O binding energy from 895 meV at 4 °K to 886 meV at 87 °K suggests that the O level is rigidly fixed to the valence band over the range $4 \leq T \leq 87$ °K. This is consistent with recent evidence^{18,19} that the electron binding energy associated with the Zn-O isoelectronic center, responsible for the high-efficiency red luminescence in GaP(Zn, O), also decreases with increasing temperature, i.e., from 300 to 230 meV in going from 4 °K to room temperature.

IV. NONRADIATIVE RECOMBINATION

In this section, elaboration is made concerning the observation that not all electrons trapped at O centers as a result of the photoneutralization process recombine radiatively. This is seen, for example, in Figs. 5 and 6 where the total infrared luminescence (the area under each spectrum in Figs. 1 and 2) is plotted as a function of tempera-

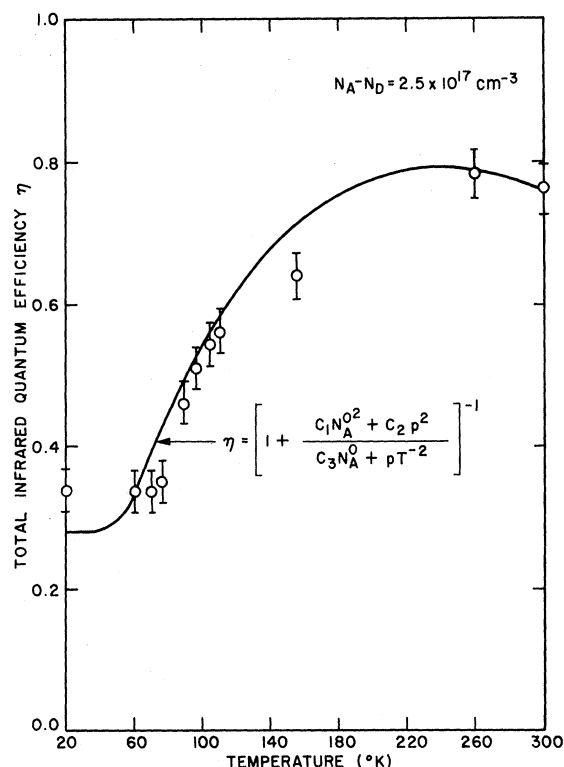


FIG. 6. Temperature variation of the total infrared emission from the lightly zinc-doped sample. The open circles represent the relative areas under the spectra in Fig. 1. The solid curve is plotted using Eq. (12) with the values $C_1 = 9.6 \times 10^{-23} \text{ cm}^3 \text{ }^\circ\text{K}^{-2}$, $C_2 = 1.6 \times 10^{-23} \text{ cm}^3 \text{ }^\circ\text{K}^{-2}$, and $C_3 = 8.8 \times 10^{-6} \text{ }^\circ\text{K}^{-2}$.

ture for both the lightly and heavily doped samples. Under low-level excitation the total infrared recombination rate is given by

$$L_{ir} = (\tau_o / \tau_{ir}) I \sigma_\alpha N_o, \quad (6)$$

where τ_o is the total lifetime of an electron trapped at an O center, τ_{ir} is the radiative lifetime, and I is the excitation intensity. Since the photoneutralization cross section σ_α has been found to be temperature independent,⁷ the temperature variations in Figs. 5 and 6 result from variations in the branching ratio¹⁸ τ_o / τ_{ir} , which for this case is just the infrared quantum efficiency η_{ir} . For the heavily doped sample (Fig. 5), some nonradiative process exists to make this ratio less than unity at higher temperatures, while in the lightly doped crystal (Fig. 6) the efficiency is quenched by some nonradiative mechanism at low temperatures. Discussed below are several possible nonradiative transitions that qualitatively explain both the doping and temperature dependence of the observed quenching.

Because of the comparatively large energy to be dissipated ($\sim 1.4 \text{ eV}$) the most likely nonradiative mechanism quenching the oxygen luminescence is

the Auger or impact recombination process.²⁰ Four possible Auger processes involving the neutral oxygen donor are shown schematically in Fig. 7, along with the two radiative mechanisms discussed in the previous sections. Process PP (the so-called T_4 process of Landsberg *et al.*²¹) is a particular example of nonradiative recombination involving the interaction of two free carriers with a third particle trapped at a single imperfection center in the crystal. Calculations of the transition rate of the PP process have been made by Landsberg *et al.*,²¹ and more recently by Sinha and DiDomenico.¹⁰ This process has been found¹⁸ to be important in explaining the temperature dependence of the decay time²²

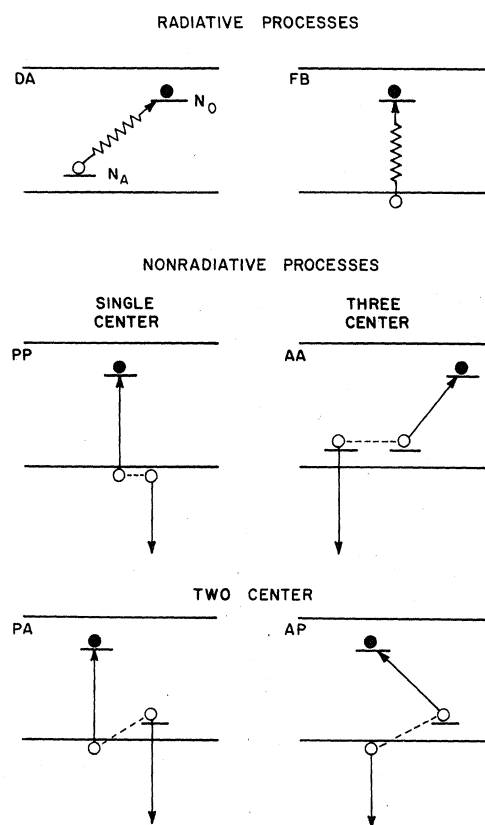


FIG. 7. Radiative and nonradiative recombination processes at the neutral oxygen donor in *p*-type GaP. An electron trapped at the oxygen donor (concentration N_o) may recombine radiatively with a hole on a neutral acceptor impurity (concentration N_A) via a DA transition, or with a free hole by means of the FB transition. Non-radiative Auger recombination of the electron interacting with two holes can be classified according to the number of separate centers involved. In the single-center process (PP), the electron interacts with two free holes, while in the three-center process (AA) the electron interacts with holes trapped on two separate acceptor impurities. Two-center recombination involves the interaction of the electron with one free hole and one trapped hole, and can be classified according to whether the recoil particle is initially trapped (PA) or free (AP).

of the efficient red luminescence originating from deep isoelectronic traps due to Zn-O nearest-neighbor pairs in GaP. It is also important in understanding the doping dependence of the room-temperature quantum efficiency and decay time of the red luminescence.^{18,19} As will be shown below, the PP process is responsible for the quenching of the infrared luminescence from neutral oxygen at higher temperature in the heavily doped sample. It can be thought of as a nonradiative analog of FB recombination, with the energy given off in the capture of the free hole being used to eject a second free hole deep into the valence band. The recombination rate for the PP process is proportional to the neutral oxygen concentration and the square of the hole concentration:

$$r_{PP} = B_{PP} p^2 N_O^0. \quad (7)$$

Thus, it possesses the proper temperature dependence to explain the data in Fig. 5, i. e., r_{PP} becomes large at high temperature where holes are thermalized off of zinc acceptors.

Auger processes involving carriers localized at two separate centers in the crystal are denoted by PA and AP in Fig. 7. Process PA is similar to the two-center problem discussed by Tolpygo *et al.*,²³ who considered capture of a minority carrier with the simultaneous ejection of a majority carrier from a neighboring center into the nearest band. The latter process is identical to that discussed by Dean and Henry³ to explain the quenching of the capture luminescence (~ 0.84 eV) for the ionized O donor. More appropriate to the experiments described here, for which no minority carriers are generated,²⁴ is the capture of *majority* carriers by the neutral O donor with the simultaneous ejection of a carrier (of either sign) from a nearby center, as in the PA process of Fig. 7. This process is also a nonradiative analog of the FB process, with the recoil particle in this case being initially bound to a shallow acceptor. The other two-center process AP is a nonradiative analog to DA pair recombination. Thus, the excess energy from the recombination of an electron trapped at a neutral O center with a hole trapped on a neutral acceptor is used in ejecting a free hole deep into the valence band. Both processes PA and AP are expected to be important in an intermediate temperature range for which the populations of free holes and neutral acceptors are comparable. The recombination rates for these transitions can be written

$$r_{PA} = B_{PA} p N_A^0 N_O^0, \quad (8a)$$

$$r_{AP} = B_{AP} p N_A^0 N_O^0, \quad (8b)$$

where use has been made of the approximations given in the Appendix.

A new⁵ type of nonradiative recombination mech-

anism involving carriers bound to three separate centers is the process AA shown in Fig. 7. This process is also a nonradiative analog of the DA transition, with the recoil particle initially bound to a shallow acceptor. The recombination rate for this process (see the Appendix) is given by

$$r_{AA} = B_{AA} N_A^0 N_O^0. \quad (9)$$

Thus, the three-center Auger process is expected to be strong at low temperatures where all the holes are frozen out onto neutral acceptors. The quenching of the low temperature infrared luminescence in the lightly doped sample (Fig. 6) can be attributed to this process.

In order to fit the data of Figs. 5 and 6, Eqs. (1), (2), and (6)–(9) can be combined to yield an expression for the infrared quantum efficiency:

$$\eta_{ir} = \left(1 + \frac{B_{PP} p^2 + (B_{PA} + B_{AP}) p N_A^0 + B_{AA} N_A^0 N_O^0}{B_{DA} N_A^0 + B_{FB} p} \right)^{-1}. \quad (10)$$

Rather than undertake the four-parameter fit required by Eq. (10), different limiting forms of the expression have been used in the case of high and low zinc doping, respectively. Thus, in fitting the data for the heavily doped sample in Fig. 5, it has been assumed that only the FB radiative and PP nonradiative processes are important, yielding the following simplification of Eq. (10):

$$\eta_{ir} = [1 + (B_{PP}/B_{FB}) p]^{\frac{1}{2}}. \quad (11)$$

In order to explain the rapid falloff of η_{ir} at higher temperatures, where the hole concentration begins to saturate, it is necessary to choose $B_{PP}/B_{FB} = CT^2$, where $C = 3.2 \times 10^{-23} \text{ cm}^3 \text{ }^\circ\text{K}^{-2}$. The T^2 dependence is not completely understood. Landsberg *et al.*²¹ find that B_{PP} increases approximately linearly with increasing temperature in the so-called first-order approximation. Assuming this dependence is correct, the observed thermal quenching of η_{ir} is explained by taking $B_{FB} \propto T^{-1}$. This inverse temperature dependence is stronger than usually calculated for a FB transition.²⁵ Since most calculations of FB transition rates^{17,26–28} involve approximations appropriate to impurities of moderate or shallow depth in direct-gap semiconductors, it is not surprising that they do not give a good account of the FB temperature dependence for the deep O donor in indirect-gap GaP.

There is clearly considerable uncertainty as to how the observed temperature dependence of B_{PP}/B_{FB} for the heavily doped sample should be divided between the PP or FB transition. For convenience we arbitrarily assign the full T^2 dependence to the FB process. Hence, we take $B_{FB} = CT^{-2}$, where C is a constant. To fit the data for the lightly doped crystal, the two-center processes are neglected,

and Eq. (10) is written in the form

$$\eta_{ir} = \left(1 + \frac{C_1 p^2 + C_2 N_A^0}{C_3 N_A^0 + T^{-2} p} \right)^{-1}, \quad (12)$$

where $C_1 = B_{PP}/C$, $C_2 = B_{AA}/C$, and $C_3 = B_{DA}/C$. From Fig. 3 we have for $N_A - N_D = 2.5 \times 10^{17} \text{ cm}^{-3}$, $r_{FB} = r_{DA}$ at $T \approx 80^\circ \text{K}$, which yields $C_3 = 8.8 \times 10^{-6} \text{ }^\circ \text{K}^{-2}$. The data in Fig. 6 are fit by adjustment of C_1 and C_2 to the values $C_1 = 9.6 \times 10^{-23} \text{ cm}^3 \text{ }^\circ \text{K}^{-2}$ and $C_2 = 1.6 \times 10^{-23} \text{ cm}^3 \text{ }^\circ \text{K}^{-2}$.

The fits to the data in Figs. 5 and 6, though in good agreement with observation, are by no means quantitative. For example, the inflection point at 120°K in the data for the heavily doped crystal (Fig. 5) indicates the importance of processes other than the two (FB and PP) used in deriving Eq. (11). It does appear, however, that the single-center Auger process is the dominant recombination mechanism in this sample above 200°K . Even in the lightly doped crystal, the PP mechanism becomes important near room temperature, where it is responsible for the slight decrease in η_{ir} as T is increased from 260 to 300°K . For this sample, the infrared efficiency is quenched at a constant value over the range $20 \leq T \leq 60^\circ \text{K}$, a result that is qualitatively explained by the temperature independence of the three-center (AA) process for these temperatures. The importance of this process for the *lightly* doped sample would seem to be anomalous, since the recombination rate varies as $N_A^{0.2}$ [Eq. (9)]. To explain this result it is necessary to examine the doping dependence of the coefficients B_{AA} and B_{DA} .

Theoretical calculations show that Auger transitions of bound particles in solids have rather strong dependences on the binding energy of the trapped carrier(s). Landsberg *et al.*,²¹ for example, find that the PP process (Fig. 7) increases in strength as the binding energy of the trapped particle increases. They attribute this increase primarily to the reduction in total energy absorbed by the recoil particle as the binding energy is raised. Likewise, Tolypgo *et al.*²³ find that the transition rate of the two-center Auger process which they investigated involving two shallow centers of binding energy E_A (analogous to process AP and PA in Fig. 7) increases as E_A^2 . For processes analogous to the single-center PP mechanism, calculations by Bess²⁹ as applied to GaAs by Weisberg³⁰ also show an increasing Auger recombination rate as the binding energy increases. Likewise, Sinha and DiDomenico¹⁰ have shown that the Auger recombination rate of trapped excitons with free holes is proportional to $E_h^{5/2} E_e^{5/2}$, where E_h and E_e are the binding energies of the majority- and minority-carrier components of the exciton, respectively. By comparing the matrix element M_x for this process with that for the AA process $M_{AA}(R_1, R_2)$, and making the identifications $E_h \rightarrow E_A$, $E_e \rightarrow E_O$, one can show³¹ for a

suitable choice of origin

$$M_{AA}(R_1, R_2) = (1/a_A)^{5/2} e^{(-R_1 - a_0 - R_2/R_s)} M_x, \quad (13)$$

where R_1 and R_2 are the separations of the two neutral acceptor atoms from the donor impurity, a_A and a_0 are the effective Bohr radii of the acceptor and donor states, respectively, and R_s is the screening length.¹⁰ Since $a_A \propto E_A^{-1/2}$, and $M_x^2 \propto E_h^{5/2} E_e^{5/2}$, we find

$$B_{AA} \propto (1/a_A)^5 M_x^2 \propto E_A^5. \quad (14)$$

The approximations leading to Eq. (14) give an upper bound to the dependence on E_A . By comparison with the two-center process we expect $B_{AA} \propto E_A^n$ where $2 \leq n \leq 5$.

Empirically³² it is found that the acceptor binding energy E_A shifts as a function of acceptor concentration according to the formula^{9,10}

$$E_A = E_A^0 - 3 \times 10^{-8} N_A^{1/3} \text{ eV}, \quad (15)$$

where E_A^0 is the dilute ionization energy ($E_A^0 = 64 \text{ meV}$ for zinc). Some workers³³ have suggested that Eq. (15) does not refer to a real shift in ionization energy, but results rather from a sensitivity of thermal activation experiments (e.g., Hall measurements) to other shallow energy states of the crystal. On the other hand, Bonch-Bruevich³⁴ has given theoretical justification for a real shift in binding energy given by Eq. (15) in terms of plasma screening of the Coulomb potential by both bound and free carriers. Taking the latter point of view, we see that Eqs. (14) and (15) predict a strong decrease in three-center Auger recombination as the zinc concentration is increased.

The factor which determines whether or not the nonradiative three-center process will be observed at low temperature is its strength relative to the radiative DA pair process, i.e., the ratio r_{DA}/r_{AA} . Using a simple atomic model it can be shown^{31,35}

$$r_{DA} \propto E_A E_O^{3/2} (E_A^{1/2} + E_O^{1/2})^{-10} N_A^0, \quad (16)$$

where E_O is the oxygen-donor ionization energy. Combining Eqs. (9) and (14)–(16), we find that if B_{AA} varies as strongly as the fifth power of E_A , then r_{DA}/r_{AA} decreases by a factor of 5 as N_A is decreased from 10^{18} to 10^{17} cm^{-3} . If these approximate calculations are valid they indicate that the three-center process in some cases can be stronger relative to pair emission in the lightly zinc-doped samples, in agreement with the experimental findings.

Although the three-center process is a plausible mechanism for explaining the low-temperature quenching in the lightly doped crystal, at least one other possibility should be mentioned. Thus, a two-center Auger process involving a multivalent acceptor³⁶ (e.g., Cu in GaP) would also explain the observed temperature dependence for the lightly doped

crystal. In this process, the electron at the neutral O site recombines with one of the holes frozen out on the acceptor, while a second hole is ejected out of the acceptor into the valence band. If such a multivalent Auger process were responsible for the observed low-temperature quenching, then the lack of quenching in the heavily doped sample could be explained chemically, on the basis of the incorporation of the unknown multivalent acceptor into the GaP lattice as a function of zinc doping. Alternatively, the reduction in E_A could also be expected to reduce the strength of the multivalent process in the more heavily doped sample in analogy with the three-center process.

V. TIME DECAY

As shown by Thomas *et al.*¹¹ the luminescent decay for a DA pair process is a nonexponential function of time, resulting from the spatial dependence of the transition probability. On the other hand, the FB process exhibits an exponential time decay for sufficiently low excitation intensities that the majority-carrier concentration is not modulated by the exciting radiation. Hence, it would appear that time-decay measurements furnish a means of distinguishing between the two radiative processes.¹² The existence of the Auger processes shown in Fig. 7 interferes with this procedure, however, since the nature of the time decay is determined by the dominant recombination mechanism, which is not necessarily a radiative one.

More explicitly, we can express the lifetime τ_0 of a carrier at the recombination center in terms of the coefficients defined previously:

$$1/\tau_0 = B_{FB}p + B_{DA}N_A^0 + B_{PP}p^2 + (B_{PA} + B_{AP})N_A^0p + B_{AA}N_A^0{}^2. \quad (17)$$

If either of the processes FB or PP dominate the lifetime, then the decay will be exponential, while the processes DA, PA, AP, and AA give rise to a nonexponential decay. As an example, consider the case for which the acceptors are 50% ionized so that $p = N_A^0$. Then, even if $B_{FB} \gg B_{DA}$, the decay will be nonexponential if we also have $B_{PA}N_A^0 \gg B_{FB}$. Thus, decay-time measurements do not necessarily furnish an unambiguous determination of the nature of the *radiative* recombination mechanism at a defect center. Only in the extreme limits (i) $p \ll N_A^0$ or (ii) $p \gg N_A^0$ do we expect a clear-cut distinction to be possible on the basis of time-decay measurements. For these limits we expect, in case (i), all dominant radiative and nonradiative transitions to be nonexponential, and in case (ii), all dominant radiative and nonradiative process to be exponential.

In the case of the oxygen donor in GaP, the analysis of Sec. IV indicates that the FB radiative and

PP nonradiative transitions dominate the recombination above $\approx 170^\circ\text{K}$ in the heavily doped *p*-type crystal (Fig. 5). Thus, we expect the time decay to be exponential above this temperature, as has been observed by Bhargava.¹² In contrast to Ref. 12, however, we find a large fraction of the total room-temperature recombination to be nonradiative for this doping level. For the lightly zinc-doped sample (Fig. 6), the fitting parameters used in Eq. (12) indicate that the AA process is important up to $\approx 220^\circ\text{K}$. Hence, we expect the infrared time decay for this crystal²⁹ to be nonexponential well above 120°K , even though the radiative transition is almost completely FB.

VI. SUMMARY

A new infrared emission band (1.45 eV) in uncompensated regions of lightly zinc-doped crystals of *p*-GaP(Zn, O) has been identified as resulting from the radiative capture of free holes by the deep neutralized oxygen donor. This transition is found to be the dominant radiative recombination process at neutral oxygen in GaP above 120°K . Two nonradiative Auger processes have been suggested to explain the quenching of the infrared luminescence. At high temperatures in the more heavily zinc-doped sample the recombination at neutral oxygen is dominated by a single-center Auger process involving the interaction of two free holes. To explain the quenching of the oxygen luminescence at low temperatures in the lightly doped sample, a new three-center Auger process is postulated. Approximate calculations indicate that the three-center process correctly explains the observed temperature and doping dependence.

ACKNOWLEDGMENTS

The author is indebted to M. DiDomenico, Jr., for a critical reading of the manuscript as well as a number of helpful discussions, including the original suggestion that the room-temperature 1.36-eV emission band results from a FB transition. The solution-grown samples were provided by F. A. Trumbore and L. Derick. The expert technical assistance of E. F. Kankowski is also gratefully acknowledged.

APPENDIX: POSITION-DEPENDENT KINETICS

Calculations of the recombination kinetics involving transitions between separated DA pairs and triplets are complicated by the spatial dependence of the transition rate. Consider a crystal in which the donor concentration N_D is dilute relative to the acceptor concentration N_A . For a given distribution $\{\vec{r}_j\}$ of acceptor positions relative to a donor at the origin, the kinetic equations can be solved straightforwardly in terms of exponential functions. The quantity of interest, however, is the ensemble aver-

age of the solution, taken over all possible distributions of $\{\tilde{r}_j\}$.¹¹ The necessity of taking ensemble averages greatly complicates the computation of the time decay—which becomes nonexponential—and the quantum efficiency. Here we investigate the approximations necessary to derive the simplified expressions given in the text, i.e., Eqs. (2), (8), and (9).

Low-level steady-state recombination at neutral oxygen (at the origin) is governed by the following equation, assuming a given distribution $\{\tilde{r}_j\}$ of acceptor positions and a photogeneration rate G :

$$G = N_O^0 \left[\sum_j [W_{DA}(r_j) + W_{PA}(r_j) + W_{AP}(r_j) + \sum_i W_{AA}(r_j, r_i)] + B_{FB} p + B_{PP} p^2 \right]. \quad (A1)$$

In Eq. (A1) the quantities $W_{DA}(r_j)$, $W_{PA}(r_j)$, and $W_{AP}(r_j)$ are the transition probabilities for an electron at the O donor to recombine with a hole on a neutral acceptor at \tilde{r}_j via processes DA, PA, and

AP, respectively. The quantity $W_{AA}(r_j, r_i)$ is the transition probability for the AA process, in which a second hole on the acceptor at \tilde{r}_i is ejected into the valence band. It will be convenient to define the quantity D via the relation $G = N_A^0 D$, by comparison with Eq. (A1). For this distribution $\{\tilde{r}_j\}$ of acceptors, the total DA recombination rate is given by

$$R'_{DA} = (G/D) \sum_j W_{DA}(r_j). \quad (A2)$$

The experimentally observed quantity is the ensemble average of R'_{DA}

$$R_{DA} = \langle R'_{DA} \rangle = \langle (G/D) \sum_j W_{DA}(r_j) \rangle. \quad (A3)$$

In general the ensemble average in Eq. (A3) is difficult to perform. We gain simplicity if we make the approximation

$$R_{DA} \approx G \langle \sum_j W_{DA}(r_j) \rangle / \langle D \rangle. \quad (A4)$$

The average $\langle \sum_j W_{DA}(r_j) \rangle$ is straightforwardly evaluated:

$$\langle \sum_j W_{DA}(r_j) \rangle = \sum_j \frac{1}{V^n} \int \dots \int W_{DA}(r_j) d^3 r_1 d^3 r_2 \dots d^3 r_j \dots d^3 r_n, \quad (A5)$$

where n is the number of neutral acceptors in the crystal volume V . Noting that $N_A^0 = n/V$, we have from Eq. (A5)

$$\langle \sum_j W_{DA}(r_j) \rangle = N_A^0 \int W_{DA}(r) d^3 r. \quad (A6)$$

If we identify $\langle D \rangle = G/N_O^0$, then combining Eqs. (A4)

and (A6), we obtain Eq. (2) in the text, where

$$B_{DA} \equiv \int W_{DA}(r) d^3 r. \quad (A7)$$

Likewise, we obtain Eqs. (8) and (9) by similar approximations, where in particular [see Eq. (9)]

$$B_{AA} \equiv \int \int W_{AA}(r_1, r_2) d^3 r_1 d^3 r_2. \quad (A8)$$

¹P. J. Dean, C. H. Henry, and C. J. Frosch, Phys. Rev. **168**, 812 (1968).

²This value is a modification of an earlier result (Ref. 1) necessitated from a revision of the sulfur-donor ionization energy [A. Onton, Phys. Rev. **186**, 786 (1969)].

³P. J. Dean and C. H. Henry, Phys. Rev. **176**, 928 (1968).

⁴A preliminary report of the present work is found in J. M. Dishman, Bull. Am. Phys. Soc. **15**, 348 (1970). On the basis of time-decay data R. N. Bhargava (Ref. 12) has also concluded that the broad infrared emission (~ 1.36 eV) at room temperature results from FB transitions at oxygen donors. In Sec. V of the present paper it is shown that time-decay measurements are not necessarily an unambiguous method for determining the nature of radiative transitions at recombination centers. Also, in contrast to Ref. 12, we find that nonradiative transitions can be a substantial fraction of the total recombination at the neutral oxygen donor in heavily doped p -type crystals at room temperature.

⁵To the author's knowledge the three-center Auger process has not been previously discussed in the literature. Calculations have been made for single-center and two-center processes, however, and these are referred to in Sec. IV.

⁶See, for example, J. F. Miller, in *Compound Semiconductors*, edited by R. K. Willardson and H. L. Goering

(Reinhold, New York, 1962), Vol. 1, Chap. 23.

⁷J. M. Dishman and M. DiDomenico, Jr. (unpublished).

⁸M. R. Lorenz, G. D. Pettit, and R. C. Taylor, Phys. Rev. **171**, 876 (1968); M. B. Panish and H. C. Casey, Jr., J. Appl. Phys. **40**, 163 (1969).

⁹H. C. Casey, Jr., F. Ermanis, and K. B. Wolfstirn, J. Appl. Phys. **40**, 2945 (1969).

¹⁰K. P. Sinha and M. DiDomenico, Jr., Phys. Rev. B **1**, 2623 (1970).

¹¹D. G. Thomas, J. J. Hopfield, and W. M. Augustyniak, Phys. Rev. **140**, A202 (1965).

¹²R. N. Bhargava, Phys. Rev. B **2**, 387 (1970).

¹³J. S. Blakemore, *Semiconductor Statistics* (Perigamon, New York, 1962).

¹⁴Such depleted regions in the substitutional O concentration have been observed in GaP(Zn, O) as-grown crystals by means of a large area photoluminescence scan technique [M. A. Fromowitz, F. Ermanis, and I. Camlibel (unpublished)].

¹⁵J. Shah, R. C. C. Leite, and J. P. Gordon, Phys. Rev. **176**, 938 (1969).

¹⁶J. S. Blakemore, Phys. Rev. **163**, 809 (1967).

¹⁷H. B. Bebb, Phys. Rev. **185**, 1116 (1969); T. H. Keil, *ibid.* **140**, A601 (1965).

¹⁸J. M. Dishman, M. DiDomenico, Jr., and R. Caruso, Phys. Rev. B **2**, 1988 (1970); J. M. Dishman and M. DiDomenico, Jr., *ibid.* **1**, 3381 (1970).

- ¹⁹J. S. Jayson, R. N. Bhargava, and R. W. Dixon, *J. Appl. Phys.* **41**, 4972 (1970).
- ²⁰See, for example, the review article by V. L. Bonch-Bruевич and E. G. Landsberg, *Phys. Status Solidi* **29**, 9 (1968).
- ²¹P. T. Landsberg, C. Phys-Roberts, and P. Lal, *Proc. Phys. Soc. (London)* **84**, 915 (1964).
- ²²J. D. Cuthbert, C. H. Henry, and P. J. Dean, *Phys. Rev.* **170**, 739 (1968).
- ²³E. I. Tolpygo, K. B. Tolpygo, and M. K. Sheinkman, *Fiz. Tverd. Tela* **7**, 1790 (1965) [*Soviet Phys. Solid State* **7**, 1442 (1965)].
- ²⁴Below $\sim 60^\circ\text{K}$ minority carriers are generated by means of a two-step process involving the oxygen donor [J. M. Dishman (unpublished)]. This is a second-order process, however, in comparison to the Auger processes discussed here.
- ²⁵A summary of several model calculations for the FB temperature dependence is found in Ref. 13. The strongest T dependence in which the transition rate decreases with temperature is for the simple hydrogenic model of Sclar and Burnstein (Ref. 26) which gives $B_{FB} \propto T^{-1/2}$.
- ²⁶N. Sclar and E. Burnstein, *Phys. Rev.* **98**, 1757 (1955).
- ²⁷D. M. Eagles, *J. Phys. Chem. Solids* **16**, 76 (1960).
- ²⁸W. P. Dumke, *Phys. Rev.* **132**, 1998 (1963).
- ²⁹L. Bess, *Phys. Rev.* **105**, 1469 (1957).
- ³⁰L. R. Weisberg, *J. Appl. Phys.* **39**, 6096 (1968).
- ³¹J. M. Dishman (unpublished).
- ³²G. L. Pearson and J. Bardeen, *Phys. Rev.* **75**, 865 (1949).
- ³³R. C. Enck and A. Honig, *Phys. Rev.* **177**, 1182 (1969).
- ³⁴V. L. Bonch-Bruевич, *Zh. Eksperim. i Teor. Fiz.* **32**, 1092 (1957) [*Soviet Phys. JETP* **5**, 894 (1957)].
- ³⁵A. Miller and B. Friedman (unpublished), as quoted in Ref. 33, find that the DA recombination rate is $W(R) \propto E_A^{5/2} E_0^{3/2} e^{-2R/a_A}$, where R is the pair separation. Integrating this expression over a random distribution of pair separations yields a total rate $r_{DA} \propto E_A E_0^{3/2}$, whose E_A dependence is the same as Eq. (16).
- ³⁶M. K. Sheinkman, *Fiz. Tverd. Tela* **5**, 2780 (1963) [*Soviet Phys. Solid State* **5**, 2035 (1963)].

Electroreflectance Spectra of CdSiAs_2 and CdGeAs_2

J. L. Shay

Bell Telephone Laboratories, Holmdel, New Jersey 07733

and

E. Buehler

Bell Telephone Laboratories, Murray Hill, New Jersey 07974

(Received 2 November 1970)

We report electroreflectance spectra for the chalcopyrite crystals CdSiAs_2 and CdGeAs_2 . These compounds are characterized by large built-in compressions and internal displacements of the As anions due to the difference in the cation covalent radii, Cd being 27% larger than Si and 21% larger than Ge. We find that CdSiAs_2 has a direct band gap at 1.55 eV. The simple quasicubic model for the crystal field splitting of the fundamental band gap in chalcopyrite crystals breaks down in CdSiAs_2 because of a contribution ($\sim 50\%$ of the compressional splitting) of opposite sign due to the difference in the pseudopotentials of the cations Cd and Si. However, the quasicubic model quantitatively explains the observed polarization dependences in terms of the measured valence band splittings. Transitions corresponding to the Λ transitions in zinc-blende crystals are not observed in CdSiAs_2 and CdGeAs_2 . Instead, a new doublet is observed for $E \perp Z$ in both crystals, and we assign this new structure to transitions at the point N in the chalcopyrite Brillouin zone.

I. INTRODUCTION

Many of the electronic and optical properties of II-IV- V_2 chalcopyrite semiconductors can be understood in terms of a simple binary-ternary analogy which emphasizes the similarity of the zinc-blende and chalcopyrite lattices.¹⁻⁵ In previous electroreflectance studies¹⁻⁴ of CdSnP_2 and ZnSiAs_2 , a simple quasicubic model accounting for the built-in compression of the chalcopyrite lattice quantitatively explained the (i) ordering, (ii) splittings, and (iii) polarization dependences for the three

transitions derived from the triply degenerate fundamental band gap $\Gamma_{15} - \Gamma_1$ in zinc-blende crystals. A quasicubic model was also constructed to explain the splittings and polarization dependences of the transitions in CdSnP_2 and ZnSiAs_2 corresponding to the Λ transitions in zinc-blende crystals. Other electroreflectance structure was attributed to pseudodirect transitions—direct transitions in chalcopyrite corresponding to indirect transitions in zinc-blende crystals which become allowed because of the doubling of the unit cell along the Z direction in chalcopyrite crystals.